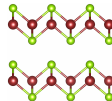


Doping dependence of superconducting transition temperatures in alkali metal/ammonia intercalated FeSe

Daniel Guterding, Harald O. Jeschke, Peter J. Hirschfeld, and
Roser Valentí
Institut für Theoretische Physik

March 4, 2015



DFG Deutsche
Forschungsgemeinschaft
SPP 1458

Superconductivity of iron selenide and derived materials

- synthesis of intercalates possible with many alkali metal/solvent combinations
- linear dependence of T_c on FeSe layer separation from 5 to 9 Å
- constant T_c beyond 9 Å
- different nominal doping levels

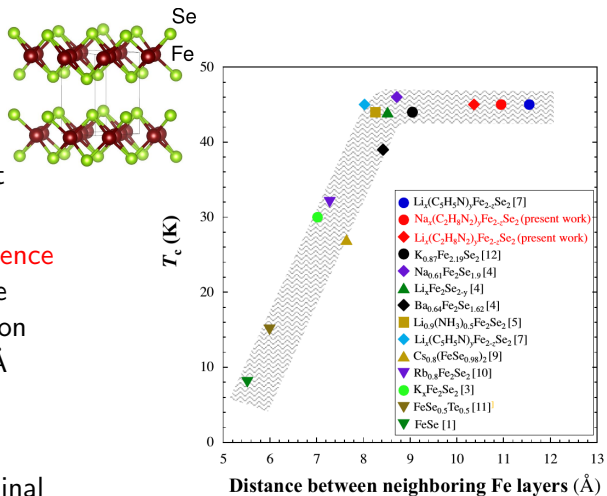


Figure : Noji et al., Physica C 504, 8 (2014)

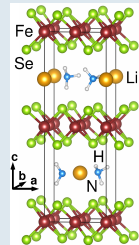
Ab-initio calculations for lithium/ammonia intercalated FeSe

Idealized structure

- $\text{Li}_x(\text{NH}_2)_y(\text{NH}_3)_z\text{Fe}_2\text{Se}_2$ with $T_c \sim 44$ K
- lattice parameters and FeSe layer from exp.

Burrard-Lucas *et al.*, Nat. Mater. **12**, 15 (2013)

Sedlmaier *et al.*, JACS **136**, 630 (2014)

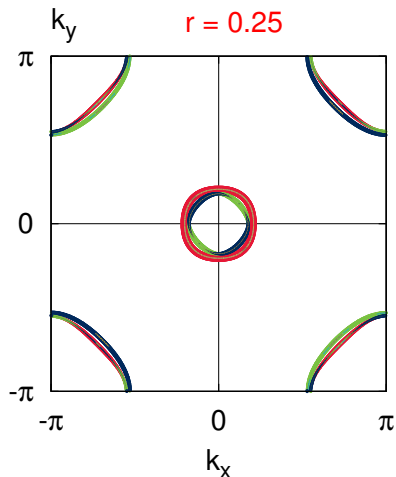
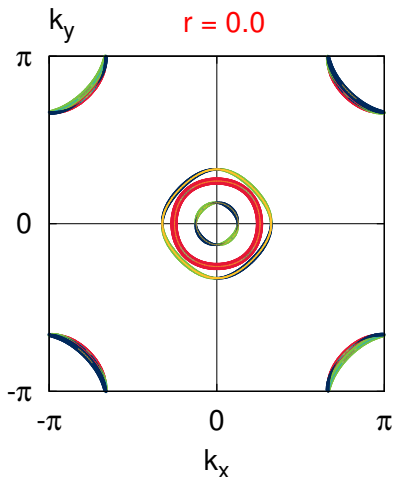


- construct super cell with Li:Fe ratio close to exp.
- result: $\text{Li}_{0.5}(\text{NH}_3)\text{Fe}_2\text{Se}_2$, 0.25 e^- per Fe doping

Electronic band structure analysis

- full potential local orbital (FPLO) code
- band structure unfolding (Tomić, Jeschke, Valentí, PRB **90**, 195121 (2014))
- projective Wannier functions (16-, 10-, 8- and 5-band models)
- simulate NH_2 with virtual crystal approximation (VCA)

Fermi surface within the 16-band model



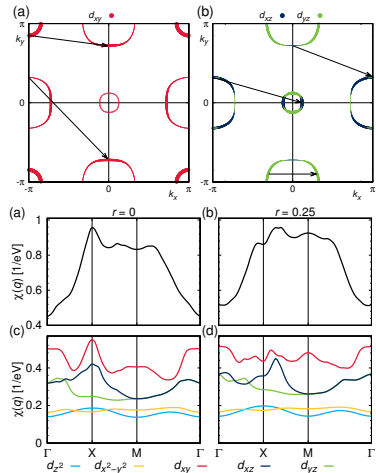
d_z^2 ● $d_{x^2-y^2}$ ● d_{xy} ● d_{xz} ● d_{yz} ●

Non-interacting susceptibility in the 8-band model

- non-interacting susceptibility reveals magnetic instabilities
- electron doping destroys $(\pi, 0)$ nesting
- **no stripe AFM** is to be expected for electron doped intercalates
- **agrees with neutron scattering exp.**

Taylor *et al.*, PRB 87, 220508 (2014)

$$\chi_{st}^{pq}(\vec{q}) = -\frac{1}{N} \sum_{\vec{k}, \mu, \nu} a_\mu^s(\vec{k}) a_\mu^{p*}(\vec{k}) a_\nu^q(\vec{k} + \vec{q}) a_\nu^{q*}(\vec{k} + \vec{q}) \frac{f(E_\nu(\vec{k} + \vec{q})) - f(E_\mu(\vec{k}))}{E_\nu(\vec{k} + \vec{q}) - E_\mu(\vec{k})}$$



RPA spin-fluctuation pairing in the 8-band model

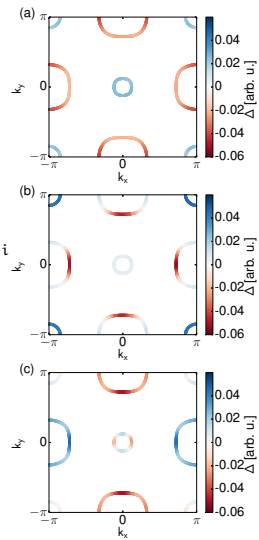
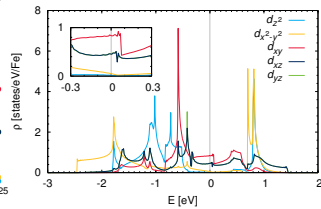
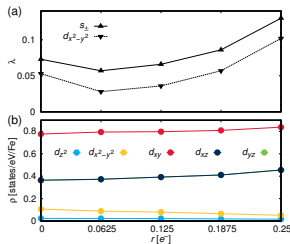
- calculate pairing interaction within random phase approximation (RPA)

Bickers, Scalapino, White, PRL **62**, 961 (1989)

Graser, Maier, Hirschfeld, Scalapino, New J. Phys. **11**, 025016 (2009)

- leading $s\pm$ instability, subleading $d_{x^2-y^2}$

$$-\sum_j \oint_{C_j} \frac{d\vec{k}'_\parallel}{2\pi} \frac{1}{4\pi v_F(\vec{k}')} \left[\Gamma_{ij}(\vec{k}, \vec{k}') + \Gamma_{ij}(\vec{k}, -\vec{k}') \right] g_j(\vec{k}') = \lambda_i g_i$$



Summary

- in 2D limit electron doping enhances T_c
- dimensionality and electron doping can be controlled through the interlayer chemistry
- increase of c-axis beyond 9 Å does not increase T_c **because system is already 2D**
- intercalates without hole pockets have low T_c because large DOS is somewhere below Fermi level
- published: **Guterding et al., PRB 91, 041112(R) (2015)**

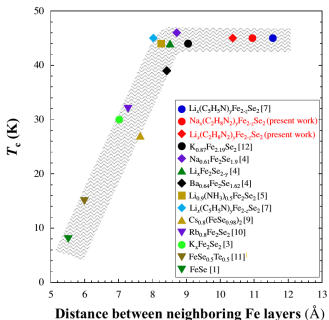


Figure : Noji et al., Physica C 504, 8 (2014)

Crystal structure and properties of lithium/ammonia intercalated FeSe

- lithium atoms are dissolved in liquid ammonia (NH_3)
- ammonia rich and ammonia poor crystals can be synthesized
- $\text{Li}_{0.56}(\text{NH}_2)_{0.53}(\text{NH}_3)_{1.19}\text{Fe}_2\text{Se}_2$ has $T_c = 39 \text{ K}$ and $c = 10.3 \text{ \AA}$
- $\text{Li}_{0.6}(\text{NH}_2)_{0.2}(\text{NH}_3)_{0.8}\text{Fe}_2\text{Se}_2$ has $T_c = 44 \text{ K}$ and $c = 8.1 \text{ \AA}$
- **larger c-axis gives lower T_c**
- $[\text{NH}_2]^-$ is a radical, should oxidize Li
- charge doping is important!

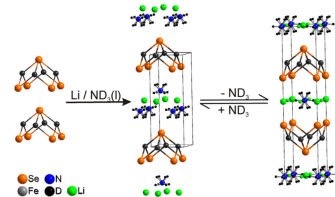


Figure : Sedlmaier et al., J. Am. Chem. Soc. **136**, 630 (2014)

Simulation of NH₂ content within VCA

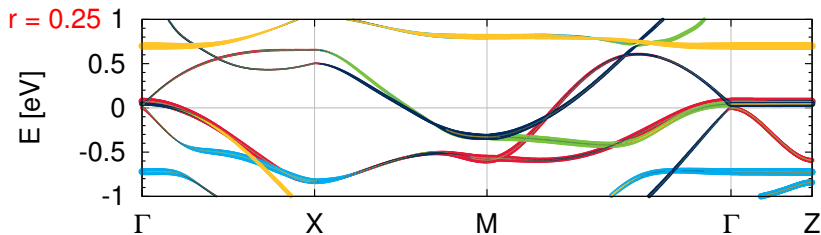
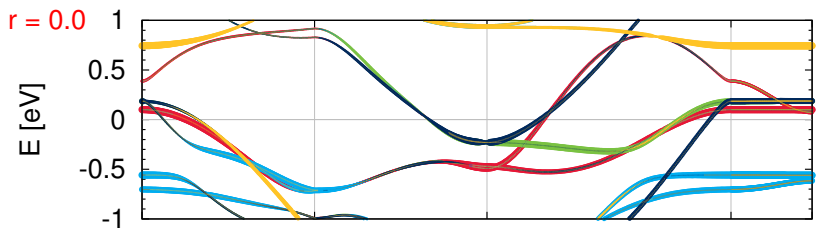
- VCA interpolates continuously between atom with nuclear charge Z and atom with nuclear charge $Z - 1$ or $Z + 1$
- fractionally replacing N ($Z = 7$) by C ($Z = 6$) **interpolates between neutral NH₃ and CH₃ radical**
- use notation
 $\text{Li}_{0.5}(\text{NH}_2)_{0.5-2r}(\text{NH}_3)_{0.5+2r}\text{Fe}_2\text{Se}_2$
- $r = \{0.0, \dots, 0.25\}$ is the **number of nominally doped e⁻/Fe**
- VCA agrees well with explicit removal of H atoms
- H bands at Fermi level then prevent good fit of band structure



$r=0.25$

$r=-0.25$

Band structure within the 16-band model



d_z^2 ● $d_{x^2-y^2}$ ● d_{xy} ● d_{xz} ● d_{yz} ●

Summary of band structure and Fermi surface analysis

Importance of NH₂

- $r = 0$ gives electronic structure like undoped material
- NH₂ content indeed controls the doping level



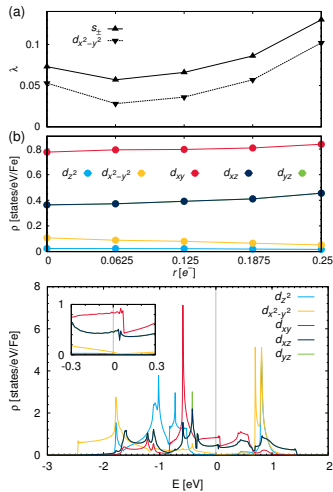
- $T_c = 39$ K and $c = 10.3$ Å
- $r = 0.015$, almost no electron doping



- has $T_c = 44$ K and $c = 8.1$ Å
- $r = 0.2$, strongly electron doped

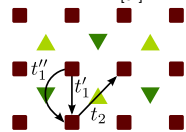
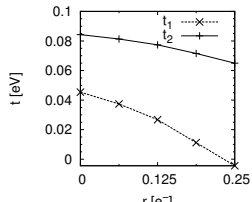
Doping dependence of the SC pairing strength

- constant interaction parameters
 $U = 1.35 \text{ eV}$, $U' = U/2$,
 $J = J' = U/4$
- pairing strength λ drops initially as nesting is destroyed, then increases with electron doping
- hole pockets are on the verge of disappearing
- electron doping increases DOS at the Fermi level
- leads to enhanced spin-fluctuations, i.e. stronger pairing
- e.g. $K_xFe_{2-y}Se_2$ has lower T_c because hole pockets are gone



Microscopic origin of the DOS enhancement

- shift of the bands is not rigid
- next-neighbor hopping in d_{xy} orbital is strongly reduced
- direct and indirect contributions to t_1 have different sign
- indirect process dominates at low doping
- states from Se are lowered in energy due to positive charge in the interlayer
- indirect hopping decreases, cancellation at maximum doping
- bandwidth reduction and Fermi level shift work together to enhance the pairing
- lower two figures adapted from Suzuki et al., PRL 113, 027002 (2014)



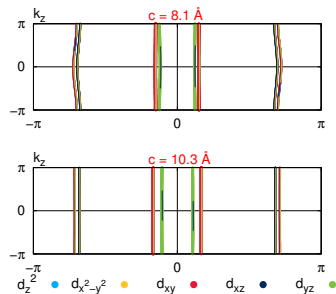
$$2t_1'' = \begin{array}{c} \uparrow \\ t_1 \\ \downarrow \end{array}$$

electron doping

$$2t_1'' = \begin{array}{c} \uparrow \\ t_1 \\ \downarrow \end{array}$$

Relative importance of c-axis height and electron doping

- doping dependence was extracted based on ammonia poor compound
- ammonia poor compound has slight corrugation on the Fermi surface cylinders
- higher c-axis makes ammonia rich perfectly 2D
- ammonia rich compound has higher λ at **identical doping level**
- in reality it has lower T_c
- **actual charge doping level makes the difference** in the 2D limit
- FS becomes 2D with c-axis of $\sim 9 \text{ \AA}$



Tight binding+RPA formalism in a nutshell

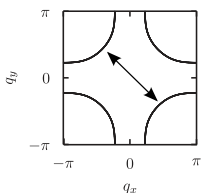
$$\chi_{st}^{pq}(\vec{q}) = -\frac{1}{N} \sum_{\vec{k}, \mu, \nu} a_\mu^s(\vec{k}) a_\mu^{p*}(\vec{k}) a_\nu^q(\vec{k} + \vec{q}) a_\nu^{t*}(\vec{k} + \vec{q}) \frac{f(E_\nu(\vec{k} + \vec{q})) - f(E_\mu(\vec{k}))}{E_\nu(\vec{k} + \vec{q}) - E_\mu(\vec{k})}$$

$$[(\chi_{\text{spin}}^{\text{RPA}})_{st}^{pq}]^{-1} = [\chi_{st}^{pq}]^{-1} - (U_{\text{spin}})_{st}^{pq}$$

$$\Gamma_{st}^{pq}(\vec{k}, \vec{k}') = \left[\frac{3}{2} U_s \chi_s^{\text{RPA}}(\vec{k} - \vec{k}') U_s + \frac{1}{2} U_s - \frac{1}{2} U_c \chi_c^{\text{RPA}}(\vec{k} - \vec{k}') U_c + \frac{1}{2} U_c \right]_{ps}^{tq}$$

$$\Gamma_{ij}(\vec{k}, \vec{k}') = \sum_{stpq} a_i^{t*}(-\vec{k}) a_i^{s*}(\vec{k}) \text{Re} \left[\Gamma_{st}^{pq}(\vec{k}, \vec{k}') \right] a_j^p(\vec{k}') a_j^q(-\vec{k}')$$

$$-\sum_j \oint_{C_j} \frac{dk_{||}}{2\pi} \frac{1}{4\pi v_F(\vec{k}')} \left[\Gamma_{ij}(\vec{k}, \vec{k}') + \Gamma_{ij}(\vec{k}, -\vec{k}') \right] g_j(\vec{k}') = \lambda_i g_i(\vec{k})$$



■ Graser, Maier, Hirschfeld, Scalapino, New Journal of Physics **11**, 025016 (2009)

Other interesting talks

- **Z5.00004** : Generalized unfolding method, **Friday 11:15 AM**, Milan Tomić